



Forbush decrease in lunar space environment observed by CRaTER on the LRO

Jongdae Sohn¹ · Suyeon Oh² · Yu Yi³ · Jaejin Lee¹

Received: 29 April 2019 / Accepted: 22 July 2019 / Published online: 7 August 2019
© Springer Nature B.V. 2019

Abstract The Lunar Reconnaissance Orbiter (LRO) launched on 16 June 2009 has seven instruments, including the Cosmic Ray Telescope for the Effects of Radiation (CRaTER). The CRaTER instrument characterizes the global lunar radiation environment and its biological impact by measuring galactic and solar cosmic rays. A Forbush decrease (FD) is a sudden decrease in the intensity of galactic cosmic rays (GCRs) recorded at the ground neutron monitor. Using the cosmic ray (CR) data from CRaTER, we identified the lunar CR events with a similar FD profile to that on Earth. Thirty-two FDs were found in the lunar space environment between June, 2009 and December, 2017, by a one-to-one correspondence with the FDs recorded at the terrestrial South Pole neutron monitor and associated interplanetary coronal mass ejections (ICMEs). The minimum GCR intensity of the main phase in the lunar space environment showed a correlation with the maximum interplanetary magnetic field strength of the associated ICME and was double the terrestrial FD magnitude. Because the FDs recorded by CRaTER were identified in space not on the ground, ICME can form an effective magnetic barrier by surrounding the Moon without interactions. The lunar space environment shows the FDs unaffected by the Earth's magnetosphere. In addition, the background intensity of GCR in the lunar space environment is anti-correlated with the solar activity.

Keywords Cosmic ray · Forbush decrease · LRO/CRaTER · South Pole neutron monitor

1 Introduction

The Lunar Reconnaissance Orbiter (LRO) was launched to establish a lunar return program for later missions to Mars and other destinations. The seven instruments in the science payload of the LRO include the Cosmic Ray Telescope for the Effects of Radiation (CRaTER) (Tooley et al. 2010). The LRO orbiter collects information on the lunar radiation environment in preparation for future human missions to the Moon.

CRaTER (Spence et al. 2010) was designed to identify the global lunar radiation environment and its biological impact. CRaTER is a stacked detector-absorber cosmic-ray telescope system for future human exploration of the solar system. CRaTER examines the effects of galactic cosmic rays (GCRs), solar energetic protons, particularly above 10 MeV, and any secondary radiation at the lunar surface on tissue equivalent plastic (TEP) by measuring the linear energy transfer spectra in lunar and deep space radiation environments.

Mazur et al. (2011) introduced a compact and highly precise micro-dosimeter mounted on the analog electronics board of the CRaTER instrument. The system measures the dose rates below one micro-rad/sec in the lunar radiation environment. Although the micro-dosimeter was not designed for scientific purposes, it effectively monitors even relatively small changes in the GCR intensity. They suggested that the micro-dosimeter can explain the dose rate at energies above 10 MeV.

Using ionization chambers, Forbush (1937) and Hess and Demmelmair (1937) first observed the decreases in the secondary cosmic-ray (CR) count rate, known as the Forbush

✉ S. Oh
suyeonoh@chonnam.ac.kr

¹ Korea Astronomy and Space Science Institute, Daejeon, South Korea

² Department of Earth Science Education, Chonnam National University, Gwangju, South Korea

³ Department of Astronomy, Space Science and Geology, Chungnam National University, Daejeon, South Korea

decrease (FD). Figure 1 shows an FD recorded at the terrestrial South Pole neutron monitor on 16 July 2017. The FD is a sudden decrease in GCR intensity observed on a ground-based neutron monitor. The FD is comprised of initial, main, and recovery phases. Hashim et al. (1972) introduced the term, the main phase, to represent the decreasing part in the GCR intensity time profile. The main phase occurs in less than half a day, whereas the recovery phase can last for several days. FDs are considered to be a blockage of GCR by intense interplanetary magnetic field (IMF) structures of the interplanetary (IP) shock sheath region and/or interplanetary coronal mass ejections (ICMEs) following the IP shocks (Parker 1961; Burlaga et al. 1981, 1982; Klein and Burlaga 1982; Zhang and Burlaga 1988; Lockwood et al. 1991; Badruddin 2002; Oh et al. 2008; Oh and Yi 2012).

FDs can be observed by not only ground-based particle detectors but also satellites and interplanetary probes. Recently, Winslow et al. (2018) examined a FD driven by a single ICME on 12 February 2014 at different space positions, such as Mercury, Earth, and Mars, using the data of several space probes. Based on their results, they then suggested that the size of the FD decreases exponentially with increasing heliocentric distance.

Although terrestrial FDs have been studied by experimental observations, the characteristics of an FD in the lunar space environment have not been reported. To develop the study by Winslow et al. (2018), who reported the FD identified by space probes, this study examined the characteristics of FDs in the lunar space environment in association with the ICMEs that drive them. The FDs observed by CRaTER in the lunar space environment were compared with those recorded at the terrestrial South Pole neutron monitor. This paper reports the measurements of FDs in the lunar space environment.

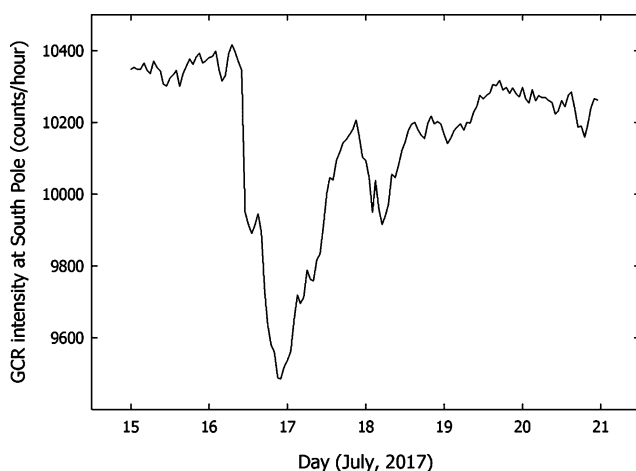


Fig. 1 Forbush decrease (FD) recorded at the terrestrial South Pole neutron monitor on 16 July 2017

2 Data and methods

The dataset from CRaTER consists of house-keeping data, primary science data, and secondary science data for Levels 0, 1, and 2. The Level-0 data were used only to renovate the other CRaTER data for archival purposes. The detector single count rate parameter of Level-2 secondary science data were provided by the CRaTER flight data of PPI (<https://pds-ppi.igpp.ucla.edu/>) and CRaTER Legacy Data Products (<http://crater-products.sr.unh.edu/>). CRaTER is comprised of six silicon detectors (D1–D6) in thin/thick pairs separated by sections of TEP. CRaTER produces a daily file with a one second resolution. The daily files report the number of ‘singles’ (silicon detector) as well as the number of ‘good’, ‘rejected’, and ‘total’ records observed by CRaTER during the monitoring period. Because ‘good’ counts are measured by the qualifying event for all count events, the hourly counter data of ‘good’ counts are used by converting the one second resolution data from June, 2009 to December, 2017. The data processing method was the same as that reported by Sohn et al. (2019). The hourly CR intensity is typically used to produce the FD profile. Because the LRO has an orbital period of 110 min, the hourly counts show oscillations with alternating highs and lows. Figure 2 in the reported by Sohn et al. (2019) compares the time resolution. Although they are averaged, the three-hour smoothed (running averaged) data have 24 intervals for each day. Because they have also been calculated by weighting, the value of each hour can maintain the original trend of the variation. The three-hour smoothed data showed a variation trend in counts because the oscillations from the orbital period are deleted. Therefore, the hourly count and dose rate data were smoothed using the three-hour weighting to determine the onset of an FD.

The three time profiles were drawn for CR intensity measured by CRaTER, dose rates by a micro-dosimeter within

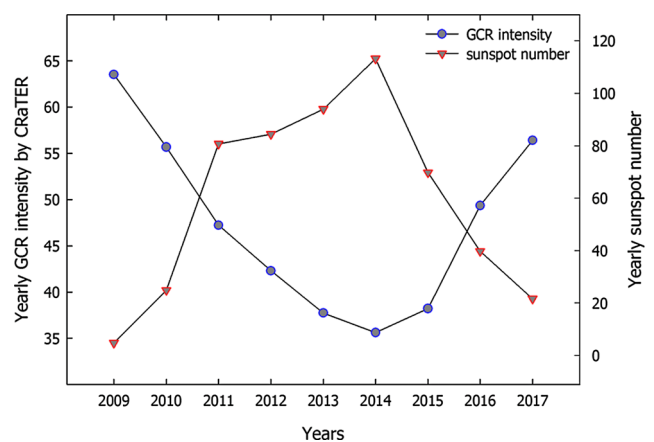


Fig. 2 Comparison of the yearly GCR intensity by CRaTER and yearly sunspot number (2009–2017). The line with circles and line with triangles indicate the GCR intensity and sunspot number, respectively

CRaTER, and CR intensity at the terrestrial South Pole neutron monitor. The associated CME lists were then selected from the SECCHI Coronagraphs onboard the STEREO satellite (<http://cor1.gsfc.nasa.gov/catalog>). The IMF data from the Magnetic Field Experiment (MAG) onboard Advanced Composition Explorer (ACE) were then compared (<http://www.srl.caltech.edu/ACE>).

This study examined the FDs with a minimum CR intensity at the main phase that is less than -2% of each GCR background in the lunar space environment. The background was defined as the average of two days before the onset of the FD. When the background was disturbed by an increasing event, we selected the quiet background before CRaTER enhancement (CRE) defined by the onset reported by Sohn et al. (2019). Thus, the CR intensity variations (%) of FDs in the lunar space environment were defined.

Figure 2 shows the yearly GCR intensity measured by CRaTER with the sunspot number from 2009 to 2017 as the long-term analysis of the CRaTER data. The line with circles and that with triangles present the GCR intensity and sunspot number, respectively. The GCR intensity in Fig. 2 indicates the background excluding the increases in CR events, such as CREs in the lunar space environment (Sohn et al. 2019). The GCR intensity in the lunar space environment was also anti-correlated with the sunspot number as an indicator of the solar activity. Figure 2 shows that the GCR intensity is affected by the solar magnetic field varying with the solar cycle because the GCR intensity is detected in space, not on the terrestrial ground. This figure shows the same results by Schwadron et al. (2012, 2014, 2018), which examined the anti-correlation between the sunspot number and dose rate using the CRaTER data.

Thirty-two FDs were identified from June, 2009 to December, 2017, in the lunar space environment. The origins and the characteristics of the FDs in the lunar space environment were examined by comparing the time profiles of CRaTER with those of the terrestrial South Pole neutron monitor and the solar wind parameters of ACE/MAG. The South Pole neutron monitor can detect neutrons produced by protons with all kinds of energy theoretically. Officially, the South Pole neutron monitor has the vertical cutoff rigidity of 0.1 GV (information of the station from NMDB, <http://www01.nmdb.eu/station/sopo/>). The cutoff rigidity of 0.1 GV is equal to the energy of 5.31 MeV. Therefore, this threshold of the South Pole neutron monitor can be comparable to that of CRaTER. To prove that the FDs observed by CRaTER are real signals, the time profile of the dose rate measured by a micro-dosimeter housed within CRaTER was also checked for any coincidence.

3 Results

Figure 3 gives an example of an FD on 18 February 2011, showing the time profiles of GCR intensity at the terrestrial South Pole neutron monitor (a), lunar GCR intensity observed by CRaTER, and lunar dose rate measured by micro-dosimeter within CRaTER (c). The time profiles of the lunar and terrestrial GCR intensity were similar and showed the typical FD, which has an initial phase, a sharp and rapid decrease in the main phase, and a gradual recovery phase. The time profile of the dose rate was similar to that of the GCR intensity. As mentioned above, the micro-dosimeter can explain the dose rate in energies above 10 MeV. The FD by CRaTER can be verified by the variation of the GCR intensity at the terrestrial South Pole neutron monitor and dose rates by CRaTER for coincidence. The minimum GCR in-

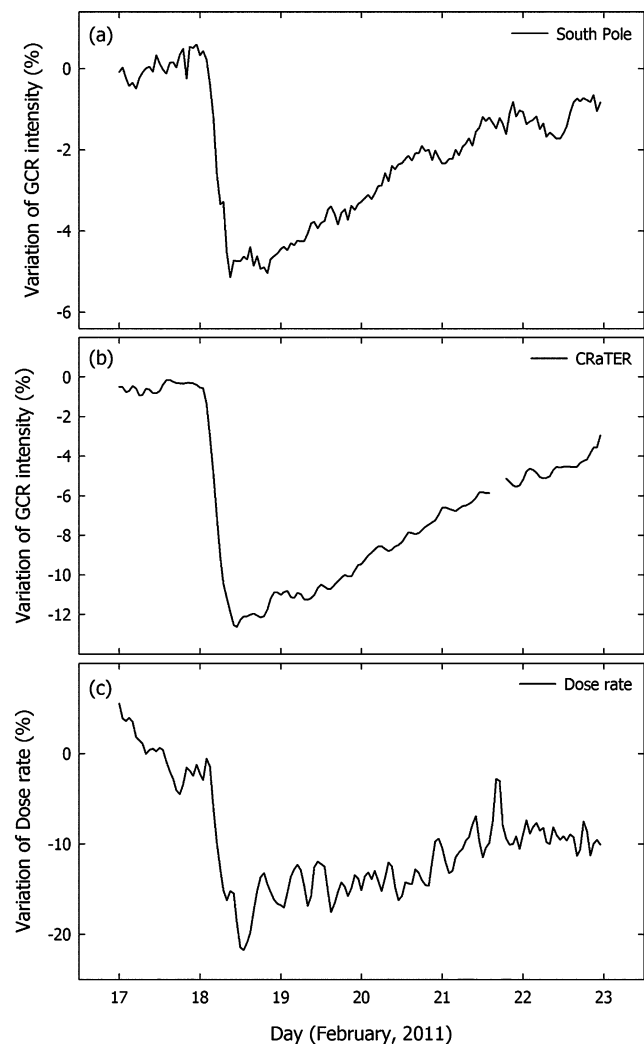


Fig. 3 Forbush decrease (FD) on the 18th of February, 2011: time profiles (a) of the GCR intensity at the terrestrial South Pole neutron monitor, (b) of GCR intensity observed by CRaTER in the lunar space environment, and (c) of the dose rate measured by the micro-dosimeter within CRaTER

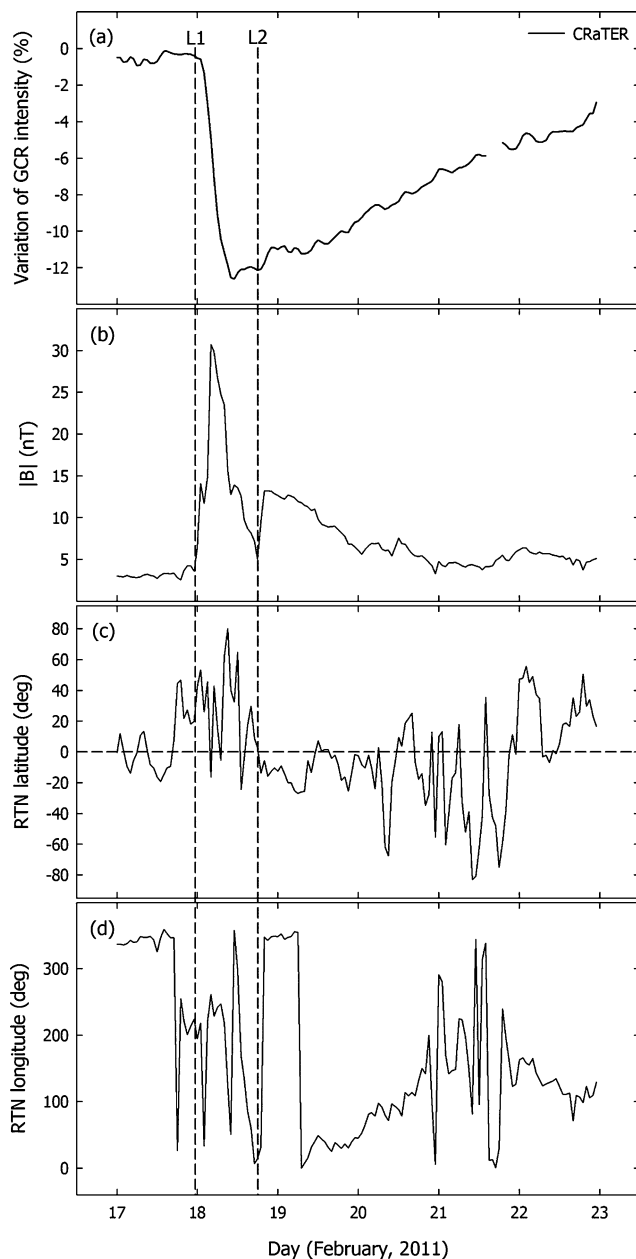


Fig. 4 ICME profiles associated with the Forbush decrease (FD) in the lunar space environment on the 18th of February, 2011: (a) time profile of the GCR intensity observed by CRaTER, (b) strength of IMF ($|B|$), (c) RTN latitude, and (d) RTN longitude. The vertical lines indicate the onset of IP shock (L1) and ICME (L2)

tensity in Fig. 3 was -5% on Earth, -12% in the lunar space environment, and the minimum dose rate was -20% in the lunar space environment. The lunar FD magnitude was double the terrestrial value.

Figure 4 shows the ICME profiles associated with FD in the lunar space environment on the 18th of February, 2011, using the IMF data measured by ACE/MAG. The figure shows the time profile of the GCR intensity observed by CRaTER (a), strength of IMF ($|B|$) (b), RTN latitude (c),

and RTN longitude (d). The vertical lines represent the onset of IP shock (L1) and ICME (L2) that drove the lunar and terrestrial FDs. The strong IMF structure of the IP shock and ICME that reached the Earth and Moon on the 18th of February, 2011, formed a strong magnetic barrier to overtake and surround both. The FDs were then recorded almost simultaneously at the terrestrial South Pole neutron monitor and CRaTER.

Figure 5 presents the lunar positions of the 32 FDs in lunar orbit according to the in/out region of the Earth's magnetosphere. Each number indicates the FD number in Table 1. Only six of these 32 FDs occur in the region of the Earth's magnetosphere in lunar orbit due to the short length of the orbit in the Earth's magnetosphere, as reported by Sohn et al. (2019). When these 32 FDs are separated into two groups based on being in or out of the Earth's magnetosphere, they show a statistically insignificant difference. This suggests that the FDs in the lunar space environment may be not influenced by the Earth's magnetosphere.

Table 1 lists the 32 FDs in the lunar space environment from June, 2009 to December, 2017. The data consist of three parts for the associated ICME, and information on the lunar (CRaTER) and terrestrial (South Pole neutron monitor) FDs. The leftmost column contains the number of the event, year, onset of ICME, and maximum IMF strength of ICME from the IMF data of ACE/MAG. For lunar FD, the table displays the date of the background, averaged count during the background period at the baseline, onset time and minimum time (the end time of the main phase), minimum GCR intensity at the minimum time, duration of the main phase, and position. The position indicates whether the point is located in or out of the Earth's magnetosphere in lunar orbit when each FD occurs. All data for terrestrial FD are displayed in the same manner as the lunar FD except for the position.

Figure 6 shows the correlation between the maximum IMF strength of the associated ICME and the minimum GCR intensity of the main phase at the terrestrial South Pole neutron monitor (a) and by CRaTER (b). The line in each panel represents the linear regression. For both the minimum lunar and the terrestrial GCR intensity of the main phase, the FD magnitude shows an increase in the negative value due to an increase in the maximum IMF strength of the associated ICME. The duration of enhanced IMF strength may also determine the FD magnitude. The lunar FD magnitude showed a slightly better correlation with the maximum IMF strength of ICME than the terrestrial value.

Figure 7 shows the correlation of the minimum GCR intensity between the lunar (CRaTER) and terrestrial (South Pole neutron monitor) main phases. Their FD magnitude showed a good correlation coefficient, but the lunar FD was double the terrestrial value. As mentioned above, the threshold of CRaTER is comparable to the cutoff rigidity of

Table 1 List of 32 Forbush decreases (FDs) in the lunar environment during the period of June, 2009 – December, 2017

Event	Year	ICME	CRaTER			Terrestrial South Pole neutron monitor											
			Maximum B (nT)	Background Date [UT] ¹	Count ²	Onset [UT]	Main phase Date [UT]	Position ³	Background Date [UT] ¹	Count ²	Onset [UT]	Main phase Date [UT]	Duration (hour)	%	Duration (hour)		
FD01	2010	Apr. 5, 5 ^h	19.7	Apr. 3, 7 ^h	56.12	Apr. 5, 8 ^h	Apr. 5, 18 ^h	Apr. 5, 18 ^h	Out	Apr. 03, 6 ^h	11365.3	Apr. 5, 7 ^h	Apr. 5, 18 ^h	-8.95	10	-3.35	11
FD02	2010	May 28, 14 ^h	14.3	May 26, 12 ^h	56.89	May 28, 13 ^h	May 28, 22 ^h	May 28, 21 ^h	In	May 26, 13 ^h	11487.3	May 28, 14 ^h	May 28, 21 ^h	-5.04	9	-3.35	7
FD03	2010	Aug. 3, 15 ^h	17.1	Aug. 1, 17 ^h	56.05	Aug. 3, 18 ^h	Aug. 4, 9 ^h	Aug. 4, 5 ^h	Out	Aug. 01, 16 ^h	11506.7	Aug. 3, 17 ^h	Aug. 4, 5 ^h	-9.95	15	-4.94	12
FD04	2010	Oct. 11, 2 ^h	13.5	Oct. 9, 2 ^h	54.77	Oct. 11, 3 ^h	Oct. 11, 23 ^h	Oct. 11, 7 ^h	Out	Oct. 09, 6 ^h	11504.9	Oct. 11, 7 ^h	Oct. 11, 21 ^h	-4.99	20	-1.83	14
FD05	2010	Oct. 22, 7 ^h	9.71	Oct. 21, 1 ^h	53.78	Oct. 23, 2 ^h	Oct. 24, 0 ^h	Oct. 23, 23 ^h	In	Oct. 20, 22 ^h	11353.9	Oct. 22, 23 ^h	Oct. 23, 23 ^h	-4.66	22	-2.17	24
FD06	2010	Nov. 27, 12 ^h	14.4	Nov. 25, 12 ^h	51.71	Nov. 27, 13 ^h	Nov. 28, 0 ^h	Nov. 28, 3 ^h	Out	Nov. 25, 17 ^h	11306.1	Nov. 27, 18 ^h	Nov. 28, 3 ^h	-3.13	11	-1.16	9
FD07	2011	Feb. 17, 23 ^h	30.7	Feb. 16, 0 ^h	54.11	Feb. 18, 1 ^h	Feb. 18, 11 ^h	Feb. 18, 9 ^h	In	Feb. 16, 0 ^h	11394	Feb. 18, 1 ^h	Feb. 18, 9 ^h	-11.17	10	-5.14	8
FD08	2011	Mar. 29, 10 ^h	14.5	Mar. 27, 13 ^h	49.51	Mar. 29, 14 ^h	Mar. 30, 9 ^h	Mar. 30, 6 ^h	Out	Mar. 27, 17 ^h	11071.5	Mar. 29, 18 ^h	Mar. 30, 6 ^h	-6.37	19	-3.35	12
FD09	2011	Apr. 5, 8 ^h	15.5	Apr. 3, 9 ^h	46.97	Apr. 5, 10 ^h	Apr. 6, 12 ^h	Apr. 6, 13 ^h	Out	Apr. 3, 9 ^h	10766.2	Apr. 5, 19 ^h	Apr. 6, 13 ^h	-8.03	26	-5.05	18
FD10	2011	Jun. 23, 0 ^h	10.3	Jun. 20, 23 ^h	45.18	Jun. 23, 0 ^h	Jun. 23, 16 ^h	Jun. 23, 0 ^h	Out	Jun. 20, 23 ^h	10605	Jun. 23, 0 ^h	Jun. 23, 21 ^h	-7.36	16	-4.95	21
FD11	2011	Jun. 23, 0 ^h	10.3	Jun. 23, 4 ^h	42.42	Jun. 24, 5 ^h	Jun. 24, 14 ^h	Jun. 24, 14 ^h	Out	Jun. 23, 4 ^h	10877.5	Jun. 23, 0 ^h	Jun. 23, 21 ^h	-3.59	4	-4.02	19
FD12	2011	Jul. 11, 7 ^h	12.8	Jul. 9, 6 ^h	46.44	Jul. 11, 7 ^h	Jul. 12, 2 ^h	Jul. 12, 3 ^h	Out	Jul. 9, 7 ^h	11021.4	Jul. 11, 8 ^h	Jul. 12, 3 ^h	-7.90	19	-4.42	24
FD13	2011	Sep. 9, 7 ^h	20.4	Sep. 4, 22 ^h	46.89	Sep. 9, 11 ^h	Sep. 10, 7 ^h	Sep. 10, 6 ^h	In	Sep. 07, 5 ^h	11004.3	Sep. 9, 6 ^h	Sep. 10, 6 ^h	-5.03	20	-6.99	12
FD14	2011	Oct. 24, 7 ^h	24.5	Oct. 20, 12 ^h	45.39	Oct. 24, 13 ^h	Oct. 25, 5 ^h	Oct. 25, 5 ^h	Out	Oct. 22, 16 ^h	10947.4	Oct. 24, 17 ^h	Oct. 25, 5 ^h	-11.87	16	-3.77	18
FD15	2011	Nov. 1, 7 ^h	12.9	Oct. 29, 4 ^h	44.68	Nov. 1, 7 ^h	Nov. 1, 23 ^h	Nov. 1, 23 ^h	Out	Nov. 30, 4 ^h	11098.6	Nov. 1, 5 ^h	Nov. 1, 23 ^h	-5.39	18	-4.68	25
FD16	2012	Jan. 22, 3 ^h	27.9	Jan. 20, 6 ^h	51.56	Jan. 22, 7 ^h	Jan. 22, 15 ^h	Jan. 23, 4 ^h	Out	Jan. 20, 2 ^h	10772.5	Jan. 22, 3 ^h	Jan. 23, 4 ^h	-7.20	8	-6.53	10
FD17	2012	Jun. 16, 18 ^h	40.4	Jun. 14, 13 ^h	45.89	Jun. 16, 21 ^h	Jun. 17, 22 ^h	Jun. 17, 5 ^h	Out	Jun. 14, 18 ^h	10512.2	Jun. 16, 19 ^h	Jun. 17, 5 ^h	-14.00	25	-4.11	7
FD18	2012	Oct. 8, 12 ^h	16.3	Oct. 6, 14 ^h	39.18	Oct. 8, 15 ^h	Oct. 8, 21 ^h	Oct. 8, 20 ^h	Out	Oct. 06, 12 ^h	10512.2	Oct. 8, 13 ^h	Oct. 8, 20 ^h	-7.47	6	-4.14	15
FD19	2012	Oct. 8, 12 ^h	16.3	Oct. 6, 14 ^h	39.18	Oct. 9, 15 ^h	Oct. 10, 5 ^h	Oct. 10, 8 ^h	Out	Oct. 06, 12 ^h	10512.2	Oct. 9, 17 ^h	Oct. 10, 8 ^h	-6.68	14	-4.14	8
FD20	2012	Oct. 12, 7 ^h	13	Oct. 6, 14 ^h	39.18	Oct. 12, 0 ^h	Oct. 12, 22 ^h	Oct. 12, 22 ^h	Out	Oct. 10, 13 ^h	10246.6	Oct. 12, 14 ^h	Oct. 12, 22 ^h	-11.47	22	-3.86	11
FD21	2012	Nov. 13, 5 ^h	22.8	Nov. 11, 4 ^h	41.79	Nov. 13, 5 ^h	Nov. 13, 15 ^h	Nov. 13, 19 ^h	Out	Nov. 11, 7 ^h	10657	Nov. 13, 8 ^h	Nov. 13, 19 ^h	-9.29	10	-5.65	14
FD22	2013	Mar. 17, 3 ^h	17.6	Mar. 11, 13 ^h	43.02	Mar. 17, 15 ^h	Mar. 18, 3 ^h	Mar. 17, 19 ^h	Out	Mar. 15, 4 ^h	10529.7	Mar. 17, 5 ^h	Mar. 17, 19 ^h	-13.83	12	-3.18	8
FD23	2013	Jun. 6, 1 ^h	13.1	Jun. 4, 8 ^h	34.92	Jun. 6, 9 ^h	Jun. 6, 23 ^h	Jun. 6, 20 ^h	Out	Jun. 4, 8 ^h	10185	Jun. 6, 12 ^h	Jun. 6, 20 ^h	-4.81	14	-3.42	11
FD24	2013	Jun. 6, 1 ^h	13.1	Jun. 4, 8 ^h	34.92	Jun. 7, 21 ^h	Jun. 8, 4 ^h	Feb. 16, 0 ^h	In	Jun. 4, 8 ^h	10255.7	Feb. 15, 13 ^h	Feb. 16, 0 ^h	-7.57	7	-5.60	29
FD25	2014	Feb. 15, 8 ^h	15.7	Feb. 13, 13 ^h	35.43	Feb. 15, 14 ^h	Feb. 16, 9 ^h	Mar. 17, 14 ^h	Out	Feb. 13, 13 ^h	10010.4	Mar. 16, 9 ^h	Mar. 17, 14 ^h	-8.91	19	-3.54	18
FD26	2015	Mar. 16, 4 ^h	33.2	Mar. 13, 8 ^h	36.16	Mar. 16, 9 ^h	Mar. 17, 15 ^h	Sep. 8, 7 ^h	Out	Mar. 13, 8 ^h	10563.7	Sep. 7, 13 ^h	Sep. 8, 7 ^h	-14.86	30	-2.93	5
FD27	2015	Sep. 7, 11 ^h	21.2	Sep. 5, 12 ^h	39.59	Sep. 7, 13 ^h	Sep. 8, 4 ^h	Jul. 20, 5 ^h	In	Sep. 5, 12 ^h	11069.8	Sep. 7, 13 ^h	Jul. 20, 5 ^h	-6.00	15	-3.16	10
FD28	2016	Jul. 19, 16 ^h	26	Jul. 18, 0 ^h	47.29	Jul. 20, 1 ^h	Jul. 20, 17 ^h	Aug. 2, 1 ^h	Out	Jul. 17, 23 ^h	11384.1	Aug. 2, 15 ^h	Aug. 2, 1 ^h	-2.90	16	-1.87	11
FD29	2016	Aug. 2, 9 ^h	24.3	Jul. 31, 9 ^h	51.52	Aug. 2, 10 ^h	Aug. 2, 23 ^h	Sep. 27, 4 ^h	Out	Jul. 31, 14 ^h	11318.8	Sep. 27, 17 ^h	Sep. 27, 4 ^h	-5.28	13	-2.63	18
FD30	2016	Sep. 27, 13 ^h	9.78	Sep. 25, 15 ^h	52.59	Sep. 27, 16 ^h	Sep. 28, 0 ^h	May 28, 7 ^h	Out	Sep. 25, 16 ^h	10168.2	May 27, 13 ^h	May 28, 7 ^h	-4.02	8	-8.34	15
FD31	2017	May 27, 13 ^h	22.5	May 25, 13 ^h	57.81	May 27, 14 ^h	May 28, 10 ^h	Jul. 16, 20 ^h	Out	May 25, 12 ^h	10348.8	Jul. 16, 7 ^h	Jul. 16, 22 ^h	-5.41	20		
FD32	2017	Jul. 16, 4 ^h	22.5	Jul. 12, 2 ^h	58.99	Jul. 16, 6 ^h	Jul. 16, 20 ^h	Jul. 16, 20 ^h	Out	Jul. 12, 2 ^h	10348.8	Jul. 16, 7 ^h	Jul. 16, 22 ^h	-15.31	14		

¹Start date of background period (49 hours)

²Averaged counts during the background period

³Position indicates whether the point is located in or out of the Earth's magnetosphere in a lunar orbit

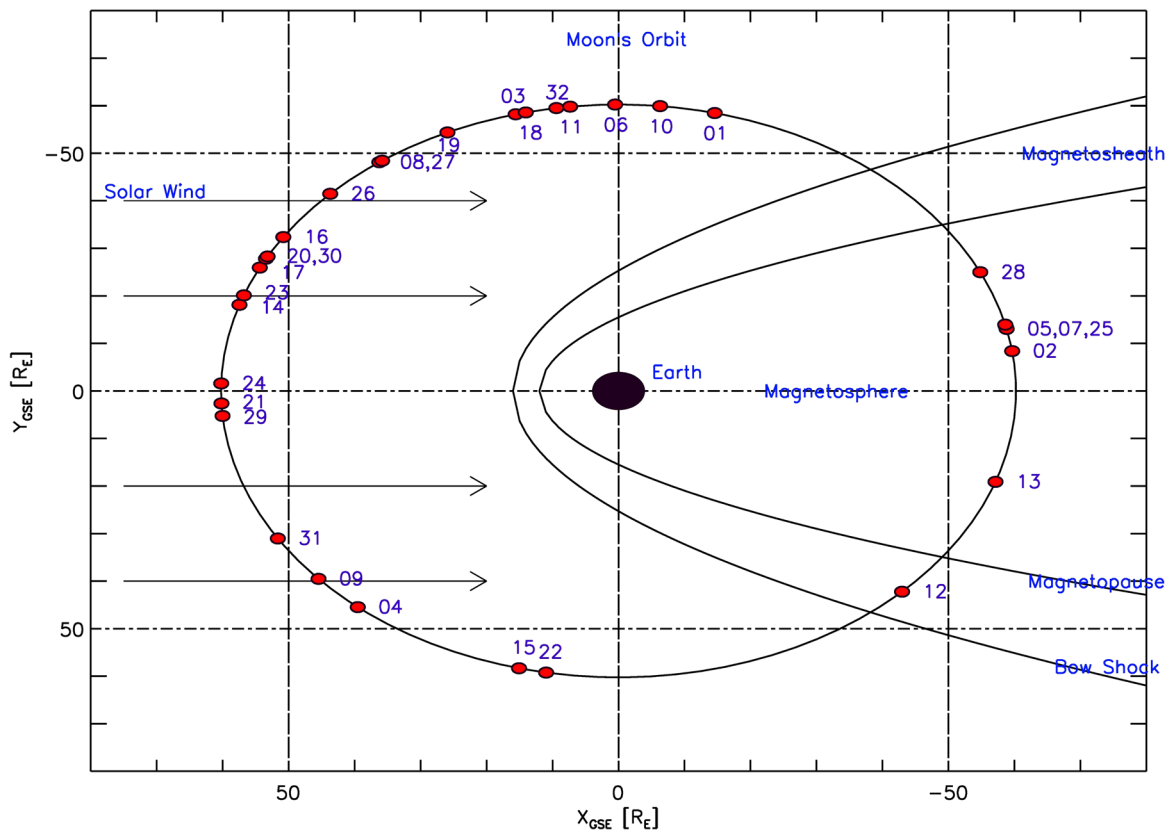


Fig. 5 Lunar positions of 32 FDs in lunar orbit according to the in/out region of the Earth’s magnetosphere. Each number indicates the FD number in Table 1

Table 2 Averaged properties of the lunar and terrestrial FD, and the associated ICME

	Maximum IMF of ICME (nT)	CRaTER		Terrestrial South Pole neutron monitor	
		Minimum GCR intensity (%)	Duration (hour)	Minimum GCR intensity (%)	Duration(hour)
Average	18.63 ± 7.33	-7.76 ± 3.48	15.25 ± 6.18	-4.08 ± 1.57	14.13 ± 6.10
Median	16.29	-7.28	15.00	-3.94	12.00
		<i>t</i>	P-value		Degrees of freedom
Student’s t-test		5.31	< 0.0001		60
Paired t-test		8.92	< 0.0001		29

the South Pole neutron monitor. Although the threshold of CRaTER is slightly larger than that of the South Pole neutron monitor, the lunar FDs have a larger magnitude than the terrestrial FDs. The orbit of the LRO is free from the Earth’s magnetic field except for the lunar position in the magnetotail of the Earth’s magnetosphere. The ICME can form an effective and strong barrier for entering CR particles in the lunar space environment without any interactions because the lunar FDs are detected by CRaTER in free space not on the ground. Table 2 lists the averaged lunar and terrestrial properties of the FD as well as the associated ICME. During the analysis period, ICME associated with FDs has a

mean IMF strength of ~ 20 nT, which is strong. The duration of the main phase shows a similar length for both lunar and terrestrial FDs. On the other hand, the minimum GCR intensity of the main phase (the lunar FD magnitude) is double that of the terrestrial value. The difference in magnitude between the terrestrial and lunar FDs was examined statistically using a Student t-Test and Paired t-Test. At a significance level of 0.05, the magnitudes of the terrestrial and lunar FDs showed a significant difference between the two groups and between each FD event. This result is presented in the last row of Table 2 and agrees with the results in Fig. 7.

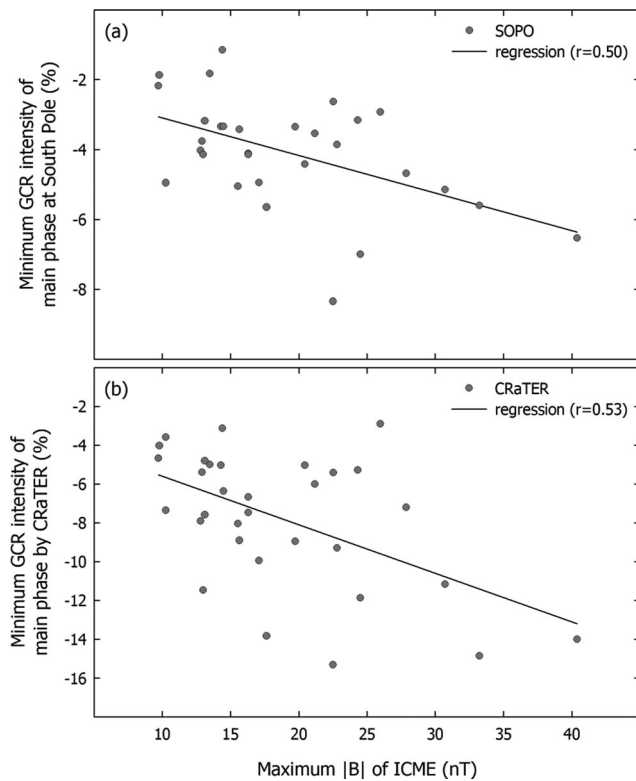


Fig. 6 Comparison between the maximum IMF strength of the associated ICME and minimum GCR intensity of the main phase: (a) minimum GCR intensity of the main phase at the terrestrial South Pole neutron monitor, and (b) minimum GCR intensity of the main phase by CRaTER

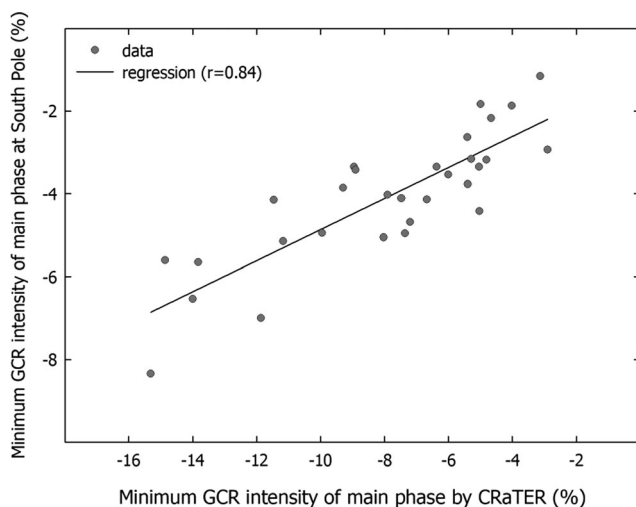


Fig. 7 Comparison of the minimum GCR intensity of lunar (CRaTER) and terrestrial (South Pole neutron monitor) main phases

4 Summary

The GCR decreasing events in the lunar space environment were examined using the CR data observed by CRaTER. Thirty-two FDs were found in the lunar space environment

during the period of June, 2009 – December, 2017, by a one-to-one correspondence with FDs recorded at the terrestrial South Pole neutron monitor and the associated ICME. The lunar and terrestrial FDs were similar and showed a distinctive decreasing profile. The minimum GCR intensity of the main phase in the lunar space environment showed a correlation with the maximum IMF strength of the associated ICME that was double the terrestrial FD magnitude. ICME can form an effective and strong barrier for the entering CR particles because the lunar FDs are recorded by CRaTER in space not on the ground; hence, the lunar FDs can be strong. That is, the FDs in the lunar space environment are stronger and they are unaffected by the Earth's magnetosphere. In addition, the background lunar GCR intensity is anti-correlated with the solar activity.

During the analysis period, FDs were less frequent than CREs. Sohn et al. (2019) reported 96 CREs during the same period. The lunar space environment allows CR particles to enter without any obstacle except for the existence of ICME. This can be expressed by the bombardment of energetic particles. Although ICME reaches the lunar space environment, the preceding solar proton event can attenuate the shielding by IMF. Hence, weak FDs can be buried by CRE in the lunar space environment. These study results highlight the need for careful consideration of the space environment when planning future space missions.

Acknowledgements This study was supported by basic research funding from the Korea Astronomy and Space Science Institute. This research was supported by the Basic Science Research Program through the National Research Foundation of Korea (NRF) funded by the Ministry of Education (NRF-2018R1D1A1B07046522). Yu Yi was supported by the Basic Science Research Program through the National Research Foundation of Korea (NRF) funded by the Ministry of Education (NRF-2016R1D1A3B03933339). The authors greatly appreciate the support from the LRO/CRaTER project under contract NASA NNG05EB92C and the STEREO/SECCHI team (Goddard Space Flight Center, Naval Research Laboratory), and the ACE/MAG team. The authors also thank the directors of the South Pole neutron monitor (Bartol Research Institute; <http://www.bartol.udel.edu/gp/neutronm/>).

Publisher's Note Springer Nature remains neutral with regard to jurisdictional claims in published maps and institutional affiliations.

References

- Badruddin: *Astrophys. Space Sci.* **281**, 651–661 (2002)
- Burlaga, L.F., Sittler, E., Mariani, F., Schwenn, R.: *J. Geophys. Res.* **86**, 6673–6684 (1981)
- Burlaga, L.F., Klein, L., Sheeley, N.R. Jr., Michels, D.J., Howard, R.A., Koomen, M.J., Schwenn, R., Rosenbauer, H.: *Geophys. Res. Lett.* **9**, 1317–1320 (1982)
- Forbush, S.E.: *Phys. Rev.* **51**, 1108–1109 (1937)
- Hashim, A., Bercovitch, M., Steljes, J.F.: *Sol. Phys.* **22**, 220–234 (1972)
- Hess, V.F., Dummel, A.: *Nature* **140**, 316–317 (1937)
- Klein, L.W., Burlaga, L.F.: *J. Geophys. Res.* **87**, 613–624 (1982)

- Lockwood, J.A., Webber, W.R., Debrunner, H.: *J. Geophys. Res.* **96**, 11587–11604 (1991)
- Mazur, J.E., Crain, W.R., Looper, M.D., Mabry, D.J., Blake, J.B., Case, A.W., Golightly, M.J., Kasper, J.C., Spence, H.E.: *Space Weather* **9**, S07002 (2011). <https://doi.org/10.1029/2010SW000641>
- Oh, S.Y., Yi, Y., Kim, Y.H.: *J. Geophys. Res.* **113**, A01103 (2008). <https://doi.org/10.1029/2007JA012333>
- Oh, S.Y., Yi, Y.: *Sol. Phys.* **280**, 197–204 (2012). <https://doi.org/10.1007/s11207-012-0053-2>
- Parker, E.N.: *Astrophys. J.* **133**, 1014–1033 (1961)
- Schwadron, N.A., Baker, T., Blake, B., Case, A.W., Cooper, J.F., Golightly, M., Jordan, A., Joyce, C., Kasper, J., Kozarev, K., et al.: *J. Geophys. Res. Space Phys.* **117**, E00H13 (2012). <https://doi.org/10.1029/2011JE003978>
- Schwadron, N.A., Blake, J.B., Case, A.W., Joyce, C.J., Kasper, J., Mazur, J., Petro, N., Quinn, M., Porter, J.A., Smith, C.W., et al.: *Space Weather* **12**, 622–632 (2014). <https://doi.org/10.1002/2014SW001084>
- Schwadron, N.A., Rahmanifard, F., Wilson, J., Jordan, A.P., Spence, H.E., Joyce, C.J., Blake, J.B., Case, A.W., deWet, W., Farrell, W.M., et al.: *Space Weather* **16**, 289–303 (2018). <https://doi.org/10.1002/2017SW001803>
- Sohn, J., Oh, S., Yi, Y., Lee, J.: *J. Korean Phys. Soc.* **74**, 614–625 (2019). <https://doi.org/10.3938/jkps.74.614>
- Spence, H.E., Case, A.W., Golightly, M.J., Heine, T., Larsen, B.A., Blake, J.B., Caranza, P., Crain, W.R., George, J., Lalic, M., et al.: *Space Sci. Rev.* **150**, 243–284 (2010). <https://doi.org/10.1007/s11214-009-9584-8>
- Tooley, C.R., Houghton, M.B., Saylor, R.S. Jr., Peddie, C., Everett, D.F., Baker, C.L., Safdie, K.N.: *Space Sci. Rev.* **150**, 23–62 (2010). <https://doi.org/10.1007/s11214-009-9624-4>
- Winslow, R.M., Schwadron, N.A., Lugaz, N., Guo, J., Joyce, C.J., Jordan, A.P., Wilson, J.K., Spence, H.E., Lawrence, D.J., Wimmer-Schweingruber, R.F., et al.: *Astrophys. J.* **856**, 139 (2018). <https://doi.org/10.3847/1538-4357/aab098>
- Zhang, G., Burlaga, L.F.: *J. Geophys. Res. Space Phys.* **93**, 2511–2518 (1988)